

A Composite Soft Bending Actuation Module with Integrated Curvature Sensing

Selim Ozel, Erik H. Skorina, Ming Luo, Weijia Tao, Fuchen Chen, Yixiao Pan, and Cagdas D. Onal

Abstract—Soft robotics carries with the promise of making robots as capable and adaptable as biological creatures, but this will not be possible without the ability to perform self-sensing and control with precision and repeatability. In this paper, we seek to address this need with the development of a new pneumatically-actuated soft bending actuation module with integrated curvature sensing. We designed and fabricated two different versions of this module: one with a commercially available resistive flex sensor and the other with a magnetic curvature sensor of our own design, and used an external motion capture system to calibrate and verify the validity of these two modules. In addition, we used an iterative sliding mode controller to drive the modules through step curvature references to demonstrate the controllability of the modules as well as compare the usability of the two sensors. We found that the magnetic sensor returned noisy but accurate data, while the flex sensor was inaccurate and subject to drift but did not exhibit notable noise. Experimental results show that this phenomenon of drift from the flex sensor causes active feedback control of the bending actuator to exhibit significant positioning errors. This work demonstrates that our soft bending actuator can be controlled with repeatability and precision, and that our magnetic curvature sensor represents an improvement for use in closed-loop control of soft robotic devices.

I. INTRODUCTION

Pneumatically actuated soft robots have many exciting properties, but these properties are largely academic without the ability to perform self-sensing and control with precision and repeatability. The compliant nature of these robots, which is one of their strengths, stymies traditional efforts to sense their state due to the infinite passive degrees of freedom provided by flexible links. In addition, the dynamic behavior of soft actuators includes a nonlinear and non-trivial time delay as pressurized air is introduced through solenoid valve commands. Thus, new methods of on-board sensing and control need to be developed to allow soft robots to be used in real environments to solve practical problems.

To address a lack of proprioceptive sensing in soft robotics research, this paper introduces a soft bending actuator module with embedded curvature measurements as a solution to sensing and control challenges related to soft robots. This is a step towards autonomous soft robots with self contained modules. Integrated sensing can be achieved through Hall effect elements or resistive flex sensors embedded in the constraint layer (neutral bending axis) for curvature measurement. Figure 1 displays the parts of the proposed segment. For segment control, we previously presented a

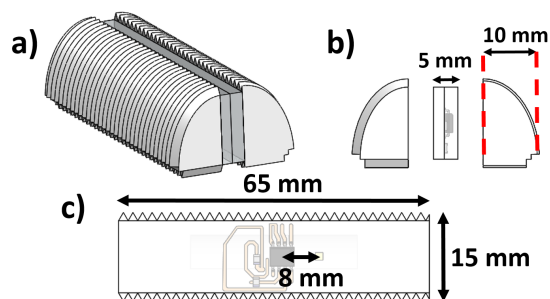


Fig. 1. Isometric (a), right (b) and front (c) views of the sensor assembly are shown. It is composed of three distinct parts: a soft bending actuator, a constraint layer in the middle of (a) and a curvature sensor. Pictured here is our custom Hall Effect sensor, though the flex sensor is fit into the same layer. Circuit tracks for our sensor are etched on a flexible sheet. A hall effect and magnet pair is used for measurements and they can be seen in (c).

hybrid-approach that used pulse width modulation (PWM) of valves to regulate pressure inside chambers [1]. Work in this paper utilizes this controller with embedded sensing to control curvature of a soft segment.

Numerous novel motions that were previously not achievable by their rigid counterparts [2], [3], [4], [5], [6], [7] were recently demonstrated using soft-bodied robot designs. We believe the field is mature enough and requires a stronger understanding of controllers, sensors and actuators that would help soft robots to achieve an increased level of autonomy. Soft robots can have very different configurations depending on the design. Indeed one advantage of soft robots is the ability to achieve relatively complex motions such as quadruped locomotion through simple designs [8]. Nevertheless, more complex tasks or locomotion in uncontrolled, open environments would eventually need feedback controllers. In this paper, we focus our attention on developing low-level curvature controllers and corresponding sensor systems appropriate for our recent soft robot designs in [9] and [10].

Accurate and embedded sensing along with a controller for regulating deformation is required for robots made out of soft bending actuators. Our snake robot in [9] is able to move without feedback control of its segments. Nevertheless, some tasks, such as finding its way through constrained environments and narrow spaces, would require some sort of feedback for motion control and planning. Visual tracking of robot configuration is a common practice in robotics. Specifically for soft-bodied robots, external motion capture may monitor the continuous kinematic configuration of the

The authors are with the Mechanical Engineering Department and Robotics Engineering Program, Worcester Polytechnic Institute, MA 01609, USA. All correspondence should be addressed to Cagdas D. Onal cdonal@wpi.edu

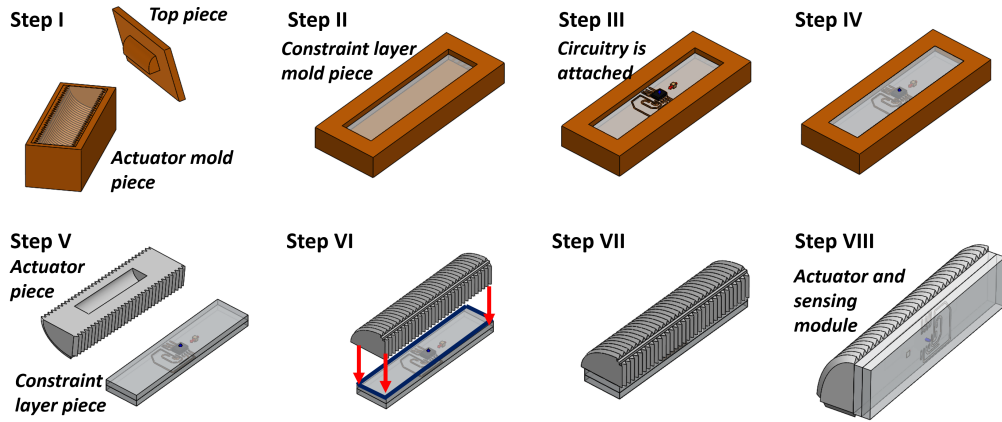


Fig. 2. Manufacturing steps of the actuator are shown in the figure. The figure shows mold designs for the actuation chamber and the constraint layer along with information on how to attach them. The actuator in Step VIII can only bend in one direction, a second actuation chamber can be attached to the opposite side for bi-directional actuation.

body. However, autonomous soft robots will require embedded sensing. Our soft robotic snake in [2] achieves serpentine locomotion patterns through actuating each segment in a predefined gait pattern to generate a traveling curvature wave that results in a forward velocity due to anisotropic friction forces at each segment. Positions of points on each segment can be defined by a single curvature value. This is due to a uniform bending moment being applied on the segment by our fluidic soft actuators [11]. Thus, kinematically stitching constant-curvature arcs, the configuration of the whole body can be obtained using curvature measurements of each segment.

There are a number of approaches to sensorizing soft bodied segments [12], [13], [14] and they also provide ways of measuring curvatures of soft bodies. For example [15] uses conductive liquids to address this issue. Finding appropriate channel geometries for required curvature ranges and manufacturing difficulties are two reasons for avoiding conductive liquids in our work. Creating channels inside silicone and injecting liquid material is a challenge. Optical fiber Bragg grating is another technology used for curvature measurements [16]. In [17] authors use light sensors along with mirrors and a light source to detect concavity and convexity to measure deflections. To achieve this, they use a sensory system with three components: Light source, a mirror and a sensor. This solution is not practical for our system. Our sensors have to be embedded inside silicone and effect of material properties on opacity and dispersion may be uncertain. We specifically pick a Hall-effect solution due to its accessibility, simple manufacturing steps, accurate response, and lack of external circuitry.

To address the forward kinematics challenge due to the design specifications of the soft snake robot, we recently developed a soft bodied curvature sensor [18]. With a magnetic operational principle, this sensor is capable of accurately measuring curvature under no external forces other than the

bending moments generated by the actuator. If gravity or other external loading is also acting on the segment, this would result in a spline-like shape for the segment, and a constant-curvature assumption would be inaccurate. Models that can approximate such splines for computing the kinematic configuration of soft bodied robots along with physical sensor systems are open research directions. Moreover, we showed that a soft layer sensorized by a magnet and a Hall effect IC can deliver accurate curvature measurements under repeated loadings as fast as 7 Hz. We verified the sensor response through numerical and analytical simulations.

To achieve a complete soft-robotic system, we integrate actuator design, soft body curvature sensing and soft actuator control. This paper develops a composite bending soft actuation module with embedded curvature sensing located at the neutral bending axis to show that such a module can be controlled reliably using on-board feedback. Throughout the paper, we will give out design and manufacturing details of this composite actuation and sensing module, and evaluate controller results from signal tracking. We utilize two different curvature sensors to verify that the accuracy offered by a commercially available, resistive flex sensor is not enough for dynamic soft robotic operation.

II. COMPOSITE SOFT BENDING MODULE

A. Actuation

We base the mechanical design of our composite module on a soft bending actuator we developed in [11]. This actuator design can endure pressures up to 10 psi. Settling time for maximum deformation is approximately 0.8 seconds. These changes are due to the addition of external threading along with a single chamber design, as opposed to serpentine air channels in our earlier work [19].

Manufacturing steps of the soft actuator and integrated sensing element are shown in Figure 2. The mechanical design is composed of several parts. Ecoflex 00-30 silicone rubber is used for the actuator body. The molds are 3D

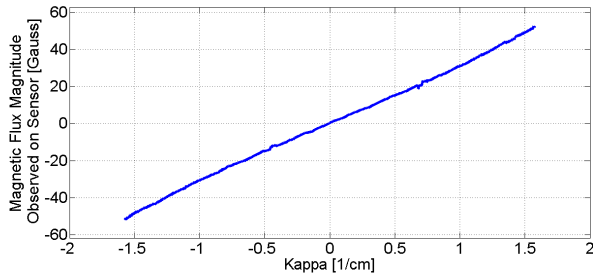


Fig. 3. Observed magnetic flux density is shown for different curvature values. Magnetic Flux Densities are obtained from finite element analysis as a look-up table. Position calculations are coded in Matlab. The distance between the magnet and the Hall element is 8 mm.

printed ABS plastic. A thread is tightly attached around the silicone structure during manufacturing to reduce radial extension. The electronic components of the sensor are built separately and they are integrated in the bidirectional bending actuator to achieve a composite module in Step III (Figure 2).

The actuator body is composed of three separately cured components. Once two circular actuators are built, threads are wrapped around them and a layer of silicone is applied over the threads. A constraint layer is cured separately. In the middle of the layer, we embed electronics on a flexible PCB to achieve a composite structure. The electronics layer is inextensible. Therefore, it also constraints the extension of the actuator assembly, assuring bending motion to be parametrized with a single curvature value.

B. Sensing

We mounted two different curvature sensors inside the constraint layers of the self contained segments in Figure 2. The first is a custom design with a Hall effect sensor and a magnet couple. The second curvature sensor consists of a commercially available resistive flex sensor.

Operational principle of the proposed magnetic curvature sensor is based on the measurement of magnetic flux densities around a magnet using a Hall element. Voltage change can be observed when a soft segment bends into different curvatures. The sensor and magnet couple are displayed in Figure 4. The sensed voltage is then inserted into a calibration function which maps voltage measurements to curvature values. This concept requires one-to-one mapping and monotonic increase to produce useful results. Magnet position and orientation settings which would result in such mapping are discovered through modeling the magnet in a finite element analysis tool and simulating the modeled parameters in a constant-curvature bending simulation of the silicone rubber segment. To show that this approach is suitable for actual implementation, we present results of a simulation in Figure 3. A more detailed discussion about this curvature sensing approach and experimental analysis of its response is provided in [18].

The magnetic curvature sensors are manufactured on custom flexible circuits using a copper tape with a printed circuit trace pattern and plastic laminate film. The copper tape

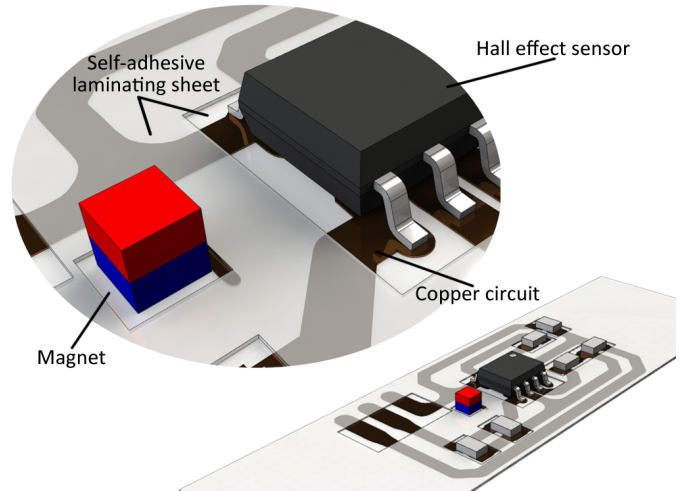


Fig. 4. An adhesive copper sheet is placed between two self laminating sheets. The top laminating sheet has laser cut holes for component placements. The assembly is passed through a lamination machine. Magnet and the hall-effect IC are shown. Red and blue color labels of the magnet indicate north and south poles respectively. Edge length of the cube magnet is 0.8 mm and overall thickness of the curvature sensing segment is 1.5 ± 0.15 mm.

is bonded onto the laminate sheet and covered by another laminate sheet layer to increase the strength of the traces for protection. Circuit component places are laser-cut on the top laminate sheet to allow for a proper fit. Figure 4 shows the detailed view of the flexible sensor. Once the flexible circuit board is completed, circuit components are populated using manual pick-and-place, which takes approximately 30 min.

As previously mentioned, an initial calibration step is required to convert the voltage measurements to curvature values. We used infrared reflective markers for tracking four points on the segment, to monitor the angle of both ends of the segment. Experimental setup for the segment with markers is shown in Figure 6. Obtaining the curvature of the segment from these four points is a simple geometric operation. We consider the visually tracked curvature values to be our baseline points for calibration. The voltage data and reference curvatures are matched in Matlab with a fourth order calibration polynomial, which can be seen in Figure 5.

The flex sensor, on the other hand, changes resistance as a function of curvature, which can be measured using a simple voltage divider given by:

$$V_o = \frac{R + C\Delta\kappa}{R + R_e + C\Delta\kappa} V_{in}, \quad (1)$$

where R is the internal resistance and it is treated as unknown. R_e is the known external resistance of the voltage divider. C is a constant parameter, which relates curvature to resistance change. C was calculated using calibration data and a least-squares fit in a similar way to our magnetic curvature sensor.

C. Control

We use miniature binary solenoid valves to control the pressure inside the actuators. The response times of these

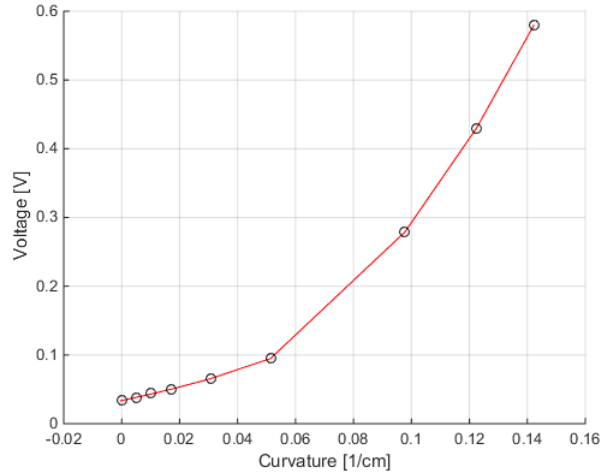


Fig. 5. Red curve is the fourth order calibration polynomial for our magnetic curvature sensor obtained from nine different dataset matches between curvatures from visual tracking and analog voltage data. Black circles represent nine different curvature data points.

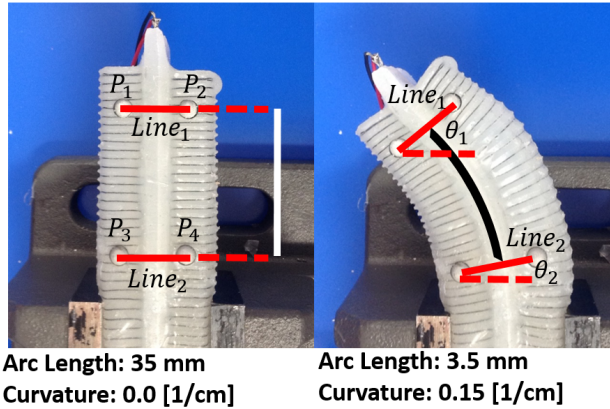


Fig. 6. The visual markers for four points are shown in the left figure. Angles of two lines segments are calculated from them. These angles can be used along with the arc length for computing curvature of the segment under circular deformations. This is the approach we implemented for calibrating the hall effect sensor through visually tracked points. The distance between top and bottom lines are 3.5 cm. The arc length does not change when the segment is actuated because the sensor layer acts as an inextensible constraint layer in the middle. When actuated with full duty cycle under 8.0 psi, segment can bend up to 0.15 [1/cm].

valves are 4 msec to fully switch between on and off states, which is sufficient for pulse width modulation (PWM) of the control signal for our experiments. The segment is driven by two actuation chambers. Incoming pressure to the chambers is controlled by regulating the PWM duty cycles of the solenoid valves with a frequency of 40 Hz. Thus, this is a system with two inputs (the PWM duty cycles on the valve of each actuator) and a single output (the curvature of the segment). For simplicity, we developed a scheme where only a single actuator was being driven at a time to reach a desired curvature value. Using this simplification, the two-actuator system could be reduced to a single control input, which

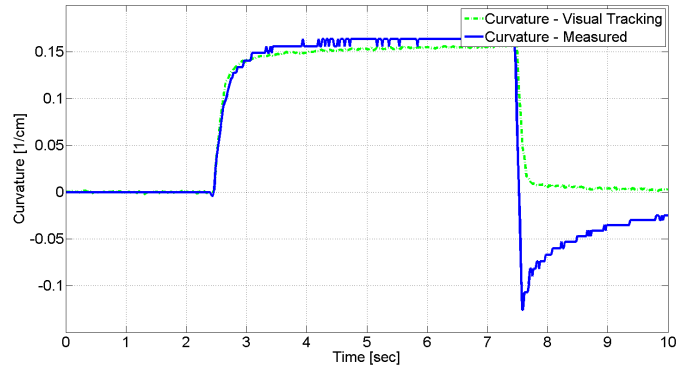


Fig. 7. Segment with the resistive flex sensor is activated for five seconds under 8 psi. Mean value of visually tracked curvature is 0.1545 cm^{-1} , when the segment is activated. Mean value of measured curvature between 2.5 – 7.5 seconds is 0.164 $\text{cm}^{-1} \pm 0.008 \text{ cm}^{-1}$. A large overshoot of approximately 75% is observed as the pressure is released.

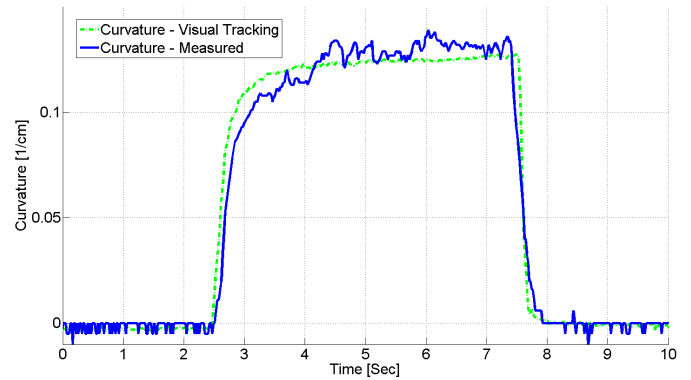


Fig. 8. In this figure, the segment with the custom magnetic curvature sensor is activated for five seconds under 8 psi. No drift is observed on the way back. Mean value of visually tracked curvature when activated is 0.1247 cm^{-1} . On the other hand mean value of curvature measurement from the magnetic curvature sensor is 0.1308 $\pm 0.015 \text{ cm}^{-1}$. No overshoot is observed.

was translated to actuation of Actuator A when positive, and Actuator B when negative.

We use a constant pressure source in our setup along with high-speed, on-off solenoid valves. We previously demonstrated that average pressure inside soft actuation chambers can be regulated through pulse width modulation (PWM) using valves [1]. Even though behavior of such control scheme is highly non-linear, our controller results were satisfactory. To control the system using the single input we adapted an iterative sliding mode controller from [1], the final control law of which is given as:

$$u(t) = u(t - \Delta t) + K(\dot{e}_x + D_x e_x), \quad (2)$$

where $u(t)$ is the control output, $u(t - \Delta t)$ is the control output from the previous time step, e_x is the error, \dot{e}_x is the derivative of the error, and K and D_x are control weights. $u(t)$ is given to the system as the PWM duty cycle and it is saturated between 0.0 – 1.0. e_x is defined as the difference between desired curvature $k_{desired}$ and $k_{measured}$.

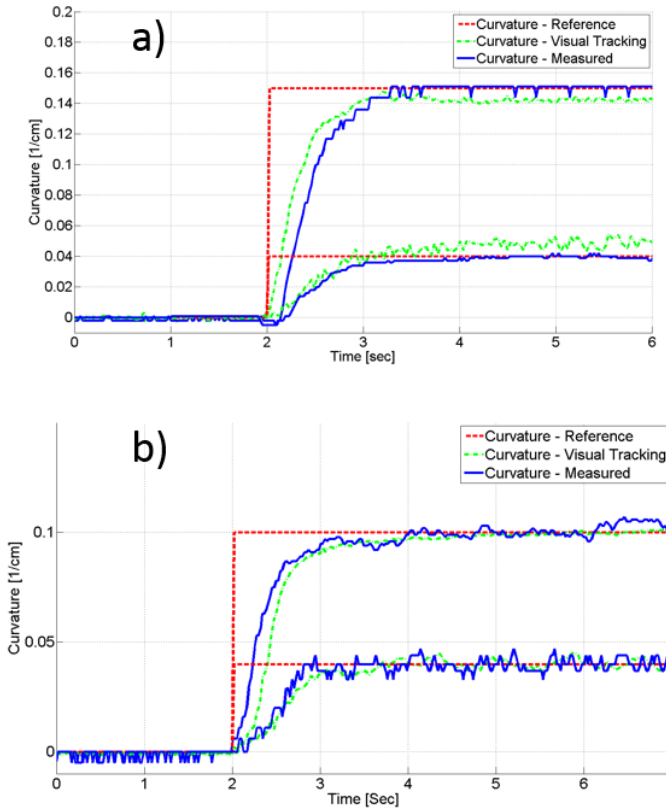


Fig. 9. Two step waves with magnitudes 0.04 cm^{-1} and 0.15 cm^{-1} are tracked using the flex sensor (a) and 0.04 cm^{-1} and 0.1 cm^{-1} with the hall effect sensor (b). A damped controller with same control gains is implemented for both sensors: $K_p = 0.25$ and $K_d = 60$. Maximum pressure is 8 psi for both of the experiments and average pressure is regulated through PWM. Feedback controller is implemented on top of PWM. Differences between visually tracked curvature and measured curvature for high amplitude step wave were 0.008 cm^{-1} for flex sensor and 0.0014 cm^{-1} for the Hall Effect sensor. The measured 5% settling time for the large step signal tracking with the Hall effect sensor is 1 sec.

III. EXPERIMENTAL RESULTS

To characterize the sensors, we performed static loading experiments to show the behavior of each sensor when actuated to a constant curvature before returning to the origin. The results of these experiments can be seen in Figure 7 for the resistive flex sensor and Figure 8 for the magnetic curvature sensor.

The flex sensor in Figure 7 seems indifferent to small changes once the actuator is pressurized up to 8 psi. This is the first limitation of using a flex sensor. Another interesting part of these experiments was when the actuator was depressurized and the segment returned to its original state. When this occurred, the Hall effect sensor followed accurately, though still exhibiting noise. The flex sensor, on the other hand, returned to a negative value of curvature nearly equal in magnitude to the pressurized curvature, before slowly settling back towards 0 to match the actual segment behavior.

From Figure 7, we can see that the flex sensor still doesn't return to reading the correct value even 2.5 seconds after the segment reached 0 curvature. In actuality, it takes 10 seconds from depressurization for the flex sensor to reach 5% of the

TABLE I

COMPARISON OF SENSORS FROM MAXIMUM PRESSURE ACTIVATION

	Flex Sensor	Magnetic Sensor
Sensor overshoot	75 %	0.0 %
Steady state measurement error [1/cm]	0.01	0.005
Peak-to-peak noise magnitude [1/cm]	0.008	0.015

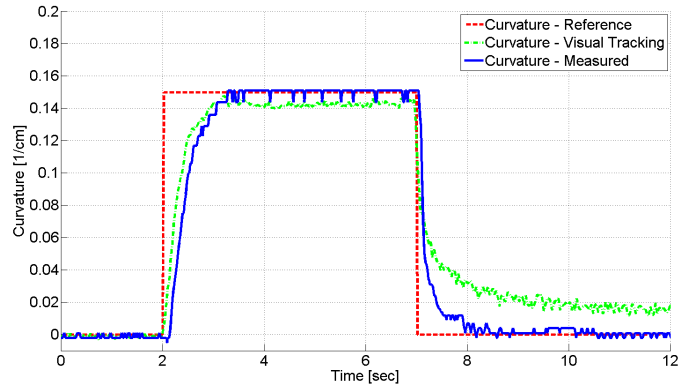


Fig. 10. Drift in the response of the flex sensor is shown during active control. The controller drives the system to zero curvature based on reference signal after 6.5 seconds. Nevertheless, the actual curvature of the segment, which is measured by the visual tracking, floats around 0.02 [1/cm] for a significant period of time.

actual value, indicating significant limitations in the accuracy of resistive measurements under dynamic conditions.

To investigate the effect of using both sensors on feedback control, we performed closed-loop control with our system using step reference curvatures for both the flex sensor and the Hall effect sensor, while simultaneously recording the curvature using external motion tracking to evaluate the accuracy of the two curvature sensing modalities. Results can be seen in Figures 9-a and 9-b for the flex sensor and magnetic curvature sensor, respectively.

These figures show that our control scheme is functional as it supplies the necessary control inputs for both segments to reach the desired curvatures based on their on-board curvature sensor measurements. The Hall effect sensor has noisy data, but it brings the segment to the correct curvature. The flex sensor, on the other hand, returns very clean but inaccurate data; its final curvature being offset from the desired by around 0.008 cm^{-1} . This offset is in different directions for the trials shown, indicating its complexity as well as highlighting the difficulty of compensating for this sensor behavior. Our quantitative analysis of the sensor responses is given in Table I.

Figure 10 shows the inconsistency between the visually tracked curvature and the sensed curvature through the flex sensor once the system is referenced to go to zero curvature. In addition, the active control test showed that the flex sensor drift caused the segment to stop short of the actual 0 curvature point by a significant margin, though less than the negative spike from the open-loop experiment in Figure 7.

IV. CONCLUSION AND DISCUSSION

This paper introduced the design, fabrication, and experimental evaluation of a new composite soft bending actuation segment with embedded curvature sensing to enable closed-loop control in soft robotics. We fabricated two different versions of this segment: one with a commercially available flex sensor and the other with a hall-effect sensor of our own design, and used a motion capture system to calibrate and verify the validity of these two sensors. In addition, we used a sliding mode controller to drive the segment through step functions to demonstrate the usability of the segments as well as compare the usability of the two sensors. We found that the segment was capable of reaching specified curvatures with speed and precision using the controller and both of the provided sensors. Moreover, we found that the Hall Effect sensor returned noisy but accurate data, while the flex sensor had an offset at steady state. When returning to the neutral position, the flex sensor showed a massive spike in the negative direction before slowly returning to the actual curvature. We performed additional experiments on this and showed that the flex sensor had still not returned to 0 after 6 seconds at steady state, and that this phenomenon caused active control of the segment to significantly undershoot when returning to the 0 curvature position. This demonstrates that our hall-effect curvature sensor represents an improvement for use in soft robot closed-loop control, though efforts should be made to reduce its noise.

One possible source of the noise in the Hall Effect sensor is the magnet placement within the sensor. In order to fit the curvature sensor inside the segment without disrupting the segment's ability to curve, the sensor was made as thin as possible, which included making the magnet as small and thin as possible as well. It is likely that the magnet did not sit well in its mount on the sensor, and that flexibility resulting in noisy data. Further work needs to be done improving the fabrication process of the segment in order to prevent this from occurring in the future.

In addition, we had numerous problems with the segments, particularly with regards to pressure leakages. The problem areas were the interfaces between the a soft bending actuator pressure chambers and the pressure lines as well as the seal between the a soft bending actuator pressure chamber and the inextensible central layer. A redesigned system for improved reliability, will allow us to perform more detailed experiments as well as use them more effectively in soft robots.

We used an iterative sliding mode controller to drive the soft segment to desired curvatures. Even though such a control scheme is useful for planar movements under no external forces, effect of gravity would significantly complicate the control system. If an external force was applied to the segment in the plane of actuation, the segment would no longer have a constant curvature. Thus, a single curvature sensor (measuring a single degree of freedom) would be unable to describe the kinematic state of the segment. A flexible array of sensors inside the segment would be needed

to reconstruct this complex shape.

REFERENCES

- [1] E. H. Skorina, M. Luo, S. Ozel, F. Chen, T. Weijia, and C. Onal, "Feedforward augmented sliding mode motion control of antagonistic soft pneumatic actuators," in *International Conference on Robotics and Automation (ICRA)*, 2015.
- [2] C. D. Onal and D. Rus, "Autonomous undulatory serpentine locomotion utilizing body dynamics of a fluidic soft robot," *Bioinspiration & Biomimetics*, vol. 8, no. 2, 2013.
- [3] L. Margheri, C. Laschi, and B. Mazzolai, "Soft robotic arm inspired by the octopus: I. from biological functions to artificial requirements," *Bioinspiration & Biomimetics*, vol. 7, no. 2, 2012.
- [4] B. Mazzolai, L. Margheri, M. Cianchetti, P. Dario, and C. Laschi, "Soft-robotic arm inspired by the octopus: II. from artificial requirements to innovative technological solutions," *Bioinspiration & Biomimetics*, vol. 7, no. 2, 2012.
- [5] A. Marchese, K. Komorowski, C. Onal, and D. Rus, "Design and control of a soft and continuously deformable 2d robotic manipulation system," in *International Conference on Robotics and Automation (ICRA)*, 2014.
- [6] M. Tolley, R. Shepherd, B. Mosadegh, K. Galloway, K. M. Wehner, Michael, R. Wood, and G. Whitesides, "A resilient, untethered soft robot," *Soft Robotics*, vol. 1, no. 3, 2014.
- [7] A. Marchese, C. Onal, and D. Rus, "Autonomous soft robotic fish capable of escape maneuvers using fluidic elastomer actuators," *Soft Robotics*, vol. 1, no. 1, 2014.
- [8] R. Shepherd, F. Ilievski, W. Choi, S. Morin, A. Stokes, A. Mazzeo, X. Chen, and G. Whitesides, "Multigait soft robot," *Proceedings of the National Academy of Sciences of the United States of America*, vol. 108, no. 51, 2011.
- [9] M. Luo, X. Pan, E. H. Skorina, W. Tao, F. Chen, S. Ozel, and C. D. Onal, "Slithering towards autonomy: A self-contained soft robotic snake platform with integrated curvature sensing," September 2015.
- [10] A. Marchese, R. Katzschmann, and D. Rus, "Whole arm planning for a soft and highly compliant 2d robotic manipulator," in *Intelligent Robots and Systems (IROS), 2014 IEEE International Conference on*, 2014.
- [11] M. Luo, W. Tao, F. Chen, T. Khuu, S. Ozel, and C. Onal, "Design improvements and dynamic characterization on fluidic elastomer actuators for a soft robotic snake," in *Technologies for Practical Robot Applications (TePRA), 2014 IEEE International Conference on*, April 2014, pp. 1–6.
- [12] R. K. Kramer, C. Majidi, and R. J. Wood, "Wearable tactile keypad with stretchable artificial skin," in *Intelligent Robots and Systems (IROS), 2011 IEEE International Conference on*, 2011.
- [13] Y. Menguc, Y.-L. Park, E. Martinez-Villalpando, P. Aubin, M. Zisook, L. Stirling, R. J. Wood, and C. J. Walsh, "Soft wearable motion sensing suit for lower limb biomechanics measurements," in *Proceedings of the International Workshop on Research Frontiers in Electronics Skin Technology at ICRA'13*, 2013.
- [14] D. M. Vogt, Y. Menguc, Y.-L. Park, M. Wehner, R. Kramer, C. Majidi, L. Jentoft, Y. Tenzer, R. Howe, and R. J. Wood, "Progress in soft, flexible, and stretchable sensing systems," in *Proceedings of the International Workshop on Research Frontiers in Electronics Skin Technology at ICRA'13*, 2013.
- [15] C. Majidi, R. Kramer, and R. J. Wood, "A non-differential elastomer curvature sensor for softer-than-skin electronics," *Smart Materials and Structures*, vol. 20, no. 10, 2011.
- [16] J. Ji, X. Zhu, L. Shen, B. Sun, and L. Jiang, "An orthogonal curvature fiber bragg grating sensor array for shape reconstruction," in *Life System Modeling and Intelligent Computing*, 2010.
- [17] M. K. Dobrzynski, I. Halasz, R. Pericet-Camara, and D. Floreano, "Contactless deflection sensing of concave and convex shapes assisted by soft mirrors," in *Proceedings of the International Workshop on Research Frontiers in Electronics Skin Technology at ICRA'12*, 2012.
- [18] S. Ozel, N. Keskin, K. D., and O. C.D., "A precise embedded curvature sensor module for soft-bodied robots," *Sensors & Actuators: A Physical (under review)*, 2014.
- [19] C. Onal and D. Rus, "A modular approach to soft robots," in *International Conference on Biomedical Robotics and Biomechatronics*, 2012.